

Quantitative imaging of nanometric optical path length modulations by time-averaged heterodyne holography in coherent frequency-division multiplexing regime.

Francois Bruno,¹ Jean-Baptiste Laudereau,¹ Max Lesaffre,¹ Nicolas Verrier,¹ and Michael Atlan¹

¹ *Institut Langevin. Fondation Pierre-Gilles de Gennes. Centre National de la Recherche Scientifique (CNRS) UMR 7587, Institut National de la Santé et de la Recherche Médicale (INSERM) U 979, Université Pierre et Marie Curie (UPMC), Université Paris 7. École Supérieure de Physique et de Chimie Industrielles - 1 rue Jussieu. 75005 Paris. France*

(Dated: December 2, 2024)

We report a demonstration of amplitude and phase imaging of out-of-plane sinusoidal vibration at nanometer scales with a heterodyne holographic interferometer. Time-averaged holograms of a phase-modulated optical field are recorded with an exposure time much longer than the modulation period. Optical heterodyning, a frequency-conversion process aimed at shifting a given radiofrequency optical side band in the sensor bandwidth, is performed with an off-axis and frequency-shifted optical local oscillator. The originality of the proposed method is to make use of a multiplexed local oscillator to address several optical side bands into the temporal bandwidth of the sensor array. This process is called coherent frequency-division multiplexing. It enables simultaneous recording and pixel-to-pixel division of two side band holograms, which permits quantitative mapping of the modulation depth of local optical path lengths yielding small optical phase modulations. Additionally, a linear frequency chirp ensures the retrieval of the local mechanical phase shift of the vibration with respect to the excitation signal, when screening a given frequency range. The proposed approach is validated by quantitative motion characterization of the lamellophone of a musical box, behaving as a group of harmonic oscillators, under weak sinusoidal excitation. Images of the vibration amplitude versus excitation frequency show the resonance of the nanometric flexural response of one individual cantilever, at which a phase hop is measured.

Imaging nanometric optical path length modulations is of interest in non-destructive testing of micro electro-mechanical systems [1]. Among common approaches used for single-point nanometric vibration spectra measurements, laser Doppler heterodyne schemes [2] are methods of choice, because of their high sensitivity and wide detection bandwidth, though imaging is hindered because scanning of the probe is required. In wide-field imaging of sinusoidal optical path length modulations, either performed with incoherent or coherent light sources, in direct image or holographic recording conditions, the mechanical phase is usually retrieved from phase-stepped stroboscopic schemes [1, 3]. In the particular case of holographic measurements, this approach is extensively used in the sinusoidal excitation regime [4–8]. Yet, in holography, the optical phase retardation of the recorded scattered field can be exploited for the determination of the local mechanical phase of an object motion with respect to the excitation signal when the readout rate of the array sensor is faster than the modulation period [9, 10]. An intermediate recording regime is quasi-time-averaging [3], for which the modulation period is of the same order of magnitude as the frame rate. Nevertheless, because the vibration frequencies of interest in non-destructive vibration screening are still much higher than camera frame rates, time-averaged interferograms [11–14] are recorded, even with high-speed cameras. Quantitative imaging of nanometer-scale optical path length modulations and phase retardation in stationary regimes, at the time scale of the frame exposure, may thus find applications.

In this letter, we report a heterodyne holographic arrangement designed for amplitude and phase imaging of nanoscale out-of-plane sinusoidal vibrations in time-averaged recording conditions without strobe light.

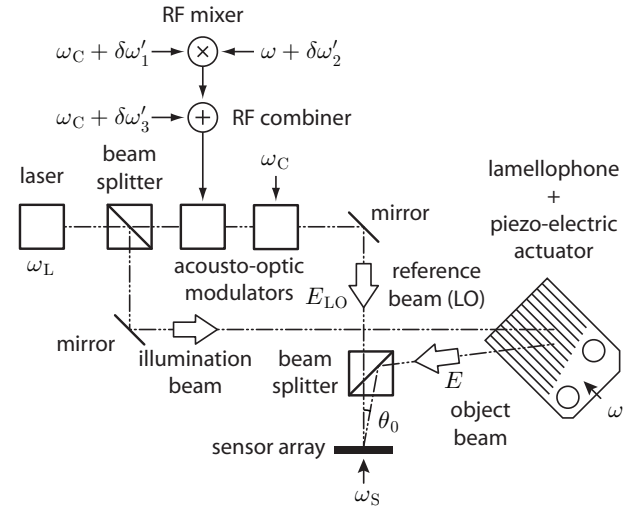


FIG. 1: Experimental set-up.

The proposed arrangement consists of a Mach-Zehnder holographic interferometer in an off-axis and frequency-shifting configuration, with a multiplexed local oscillator (fig. 1). Optical local oscillator multiplexing is realized by the coherent addition of radiofrequency (RF) signals driving an acousto-optic modulator in the reference beam channel. Coherent frequency-division multiplexing is a technique by which the total available bandwidth is divided into non-overlapping frequency sub-bands carrying separate signals. Addressing simultaneously distinct domains of the spectral bandwidth of holograms was performed with success for angular [15], wavelength [16], space-division [17], and side band [18] multiplexing schemes. Coherent frequency-division multiplexing in heterodyne holography offers the opportunity to measure complex-valued maps of the RF spectral components of

the optical radiation field with accuracy and sensitivity, as long as they can be isolated in sub bands of the sensor's temporal bandwidth. In the reported experiment, high-quality factor flexural responses at audio frequencies of a lamellophone (the metallic comb of cantilevers from a musical box) excited in a sympathetic resonance regime are sought. Sympathetic vibration is a harmonic phenomenon wherein a vibratory body responds to external excitation in the vicinity of a resonance frequency.

The optical setup used to perform non-destructive testing of the cantilevers' out-of-plane flexural responses at nanometric scales is sketched in fig.1. It is designed to screen quantitatively steady-state vibration amplitudes and to detect mechanical phase jumps with respect to the excitation signal, by interferometric detection of an optical field scattered by the lamellophone, referred to as the object field, beating against a reference optical field. The out-of-plane motion of the cantilevers provokes an optical path length modulation of the backscattered object field. Hence the temporal part of the object field E undergoes a sinusoidal phase modulation $\phi(t) = 4\pi z(t)/\lambda$. The equation of the out-of-plane motion $z(t)$ of a cantilever, modeled as a damped harmonic oscillator of spring constant k , mass m , damping coefficient c , driven sinusoidally by the force $F(t) = F_0 \sin(\omega t)$ provided by a piezo-electric actuator is

$$m \frac{\partial^2 z}{\partial t^2} + c \frac{\partial z}{\partial t} + kz = F(t) \quad (1)$$

We seek a steady-state solution at the excitation frequency with an induced phase change of ψ with respect to the excitation $F(t)$, as a result of viscous damping

$$z(t) = z_0 \sin(\omega t + \psi) \quad (2)$$

Its amplitude, z_0 , is proportional to the driving force

$$z_0 = \frac{F_0}{m\omega} \left[(2\omega_0\zeta)^2 + \frac{1}{\omega^2} (\omega_0^2 - \omega^2)^2 \right]^{-1/2} \quad (3)$$

Two intermediate variables were introduced : the angular resonance frequency ω_0 of the undamped oscillator, and the dimensionless damping ratio ζ . They satisfy the relationships $k = m\omega_0^2$ and $c = 2m\omega_0\zeta$. The phase shift of the sinusoidal response with respect to the driving force is

$$\psi = \arctan \left(\frac{2\omega\omega_0\zeta}{\omega^2 - \omega_0^2} \right) \quad (4)$$

The resonance frequencies $\omega_r = \omega_0 \sqrt{1 - 2\zeta^2}$ of each cantilever are almost equal to the resonant frequencies ω_0 of the undamped system. The optical phase modulation $\phi(t) = \phi_0 \sin(\omega t + \psi)$ of depth $\phi_0 = 4\pi z_0/\lambda$ at the angular frequency ω , can be decomposed on a basis of Bessel functions of the first kind $J_n(\phi_0)$, via the Jacobi-Anger identity

$$E = \mathcal{E} e^{i\omega_L t} e^{i\phi(t)} = \mathcal{E} e^{i\omega_L t} \sum_n J_n(\phi_0) e^{in(\omega t + \psi)} \quad (5)$$

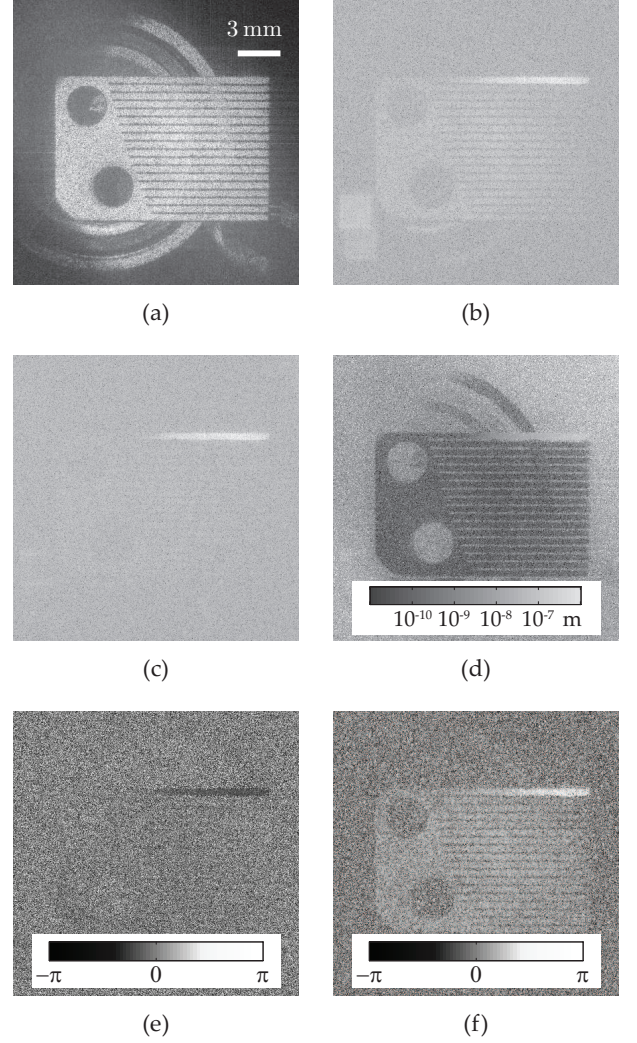


FIG. 2: Magnitude of a statically-scattered light hologram $|\tilde{H}_0|$ (a). Magnitude of side band holograms $|\tilde{H}_{-1}|$ (b) and $|\tilde{H}_1|$ (c). Amplitude map of the flexural response z_0 of the first cantilever for the first resonance at $\omega/(2\pi) = 541$ Hz (d). Phase images ψ calculated from 128 raw interferograms around 540.9 Hz (e) and 541.8 Hz (f), in the neighborhood of the first resonance. Movies of the amplitude and phase maps of the out-of-plane vibration are reported in media 1 and 2.

The quantity

$$\mathcal{E}_n = \mathcal{E} J_n(\phi_0) e^{in\psi} \quad (6)$$

is the complex weight of the optical side band of order n , where \mathcal{E} is the complex amplitude of the optical field, and $\phi_0 = 4\pi z_0/\lambda$ is the modulation depth of the optical phase of the radiation backscattered by the cantilever. The local amplitude z_0 of the out-of-plane vibration and phase retardation ψ with respect to the sinusoidal driving force can be derived from the complex weight of two optical side bands with eq. 6 and the first-order Taylor developments of $J_0(\phi_0)$ and $J_1(\phi_0)$, near $\phi_0 = 0$, for $z_0 \ll \lambda$

$$\frac{\mathcal{E}_1}{\mathcal{E}_0} \approx \frac{2\pi}{\lambda} z_0 e^{i\psi} \quad (7)$$

The holographic interferometer is used for the detection of RF phase modulation side bands of an object

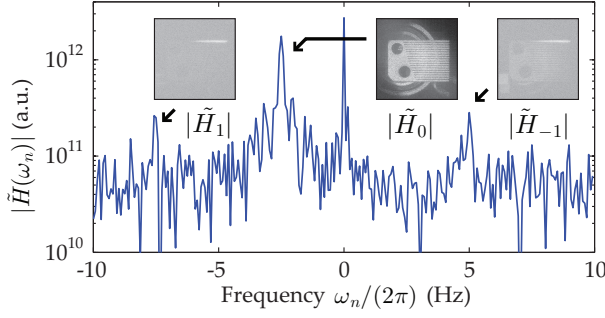


FIG. 3: Magnitude of the FFT-spectrum (eq.11 and eq. 12), where three modulation side bands are addressed.

field E in reflective geometry, beating against a LO field E_{LO} , as reported in [18]. Its purpose is to enable a robust quantitative measurement of the nanometric modulation amplitudes of cantilever resonances, as well as the associated phase shift with respect to the sinusoidal excitation signal. To do so, the adopted strategy is to separate the sensor bandwidth $[-\omega_S/2, \omega_S/2]$ into three non-overlapping frequency sub-bands, centered at $\delta\omega_1$, $\delta\omega_2$, and $\delta\omega_3$, each of which is used to carry a separate optical modulation side band. The LO signal is composed of the sum of three phase-locked RF signals, to yield an optical LO field of the form

$$E_{\text{LO}} = \mathcal{E}_{\text{LO}} e^{i\omega_{\text{L}} t} \sum_{n=1}^3 \alpha_n e^{i\Delta\omega_n t} \quad (8)$$

where $\Delta\omega_n = (n-2)\omega - \delta\omega_n$ is the frequency shift and $\alpha_n \mathcal{E}_{\text{LO}}$ is the complex weight of the LO component of rank $n = 1, 2, 3$. The positive parameters α_n are the normalized weights of each LO component; in this experiment $\alpha_1 = \alpha_2 = \alpha_3 = 1/3$. The LO components are tuned around the optical modulation bands of order -1 , 0 , and $+1$. Precisely, the LO component of rank n beats against the optical modulation band of rank $n-2$ at the apparent frequency $\delta\omega_n$, which is set within the camera bandwidth. Image rendering from the raw interferograms $\mathcal{I}(t) = |E(t) + E_{\text{LO}}(t)|^2$ impinging on the sensor array involves a diffraction calculation performed with a numerical Fresnel transform. Its implementation in off-axis holographic conditions [19] yields complex-valued time-averaged [11–14] holograms $I(t)$ from which the off-axis region

$$H(t) = E(t)E_{\text{LO}}^*(t) \quad (9)$$

is the support of the object-reference fields cross-term. The demodulation process (eq. 11) from N of consecutive recordings of finite exposure times acts as a band-pass filter of width ω_S/N in the temporal frequency domain. Only the contributions within the sensor temporal bandwidth, between the Nyquist frequencies $\pm\omega_S/2$, have to be taken into account in $H(t)$, which can hence be expressed as

$$H(t) = \sum_{n=1}^3 \mathcal{E}_{n-2} \mathcal{E}_{\text{LO}}^* \alpha_n \exp(i\delta\omega_n t) \quad (10)$$

where the quantities $\delta\omega_n$ satisfy $-\omega_S/2 < \delta\omega_n < \omega_S/2$. The FFT-spectrum of N consecutive off-axis holograms

$$\tilde{H}(\omega_n) = \sum_{p=1}^N H(2\pi p/\omega_S) \exp(-2in p\pi/N) \quad (11)$$

exhibits three peaks at the frequencies $\delta\omega_1$, $\delta\omega_2$, and $\delta\omega_3$ (fig. 3). Their complex values yield holograms \tilde{H}_m , of rank $m = -1, 0, 1$, whose magnitude is proportional the modulation depth at the frequency $\delta\omega_{m+2}$

$$\tilde{H}_m = \tilde{H}(\delta\omega_{m+2}) = A \mathcal{E}_m \quad (12)$$

where $A \propto \mathcal{E}_{\text{LO}}^* \alpha_m$ is a complex constant. Thus, \tilde{H}_m is a measure of the complex weight \mathcal{E}_m . For small-amplitude vibrations, a quantitative map of the local out-of-plane vibration amplitude z_0 can be assessed from the ratio of the first-order sideband \tilde{H}_1 and the non-shifted light component \tilde{H}_0

$$z_0 \approx \frac{\lambda}{2\pi} \left(\left| \left\langle \tilde{H}_1 / \tilde{H}_0 \right\rangle \right| \right) \quad (13)$$

where $\langle \rangle$ corresponds to spatial averaging over the extent of the resonant cantilever, arrowed in fig. 2(b). In the same manner, a map of the local mechanical phase retardation ψ with respect to the excitation signal can be assessed from \tilde{H}_1 , and \tilde{H}_0

$$\psi - \psi_0 = \text{Arg} \left(\left\langle \tilde{H}_1 / \tilde{H}_0 \right\rangle \right) \quad (14)$$

Relationships 13 and 14 are derived from eqs. 7, 12. One can also make use of the third recorded band \tilde{H}_{-1} and the property $J_{-1}(\phi_0) = -J_1(\phi_0)$ to benefit from a small SNR improvement, since we also have $z_0 \approx \frac{\lambda}{2\pi} \left(\left| \left\langle \tilde{H}_{-1} / \tilde{H}_0 \right\rangle \right| \right)$ and $\psi - \psi_0 = \text{Arg} \left(\left\langle \tilde{H}_0 / \tilde{H}_{-1} \right\rangle \right)$.

To perform the measurement, an optical LO consisting of the combination of three frequency components shifted by $\Delta\omega_1$, $\Delta\omega_2$, and $\Delta\omega_3$ (eq.8) was realized. Those shifts were chosen to yield non-symmetrical (non-opposed) algebraic modulation frequencies $\delta\omega_1$, $\delta\omega_2$, and $\delta\omega_3$ in the detector bandwidth in order to avoid spurious aliasing or cross-talk effects. To do so, we made use of phase-locked RF signals generated by frequency-synthesizers at the carrier frequency $\omega_C/(2\pi) = 80$ MHz, and $\omega_C + \delta\omega'_1$, $\omega_C + \delta\omega'_2$, $\omega_C + \delta\omega'_3$, where the shifts used to generate the three RF bands were $\delta\omega'_1/(2\pi) = -1.25$ Hz, $\delta\omega'_2/(2\pi) = 6.25$ Hz, $\delta\omega'_3/(2\pi) = -2.5$ Hz. As sketched in fig. 1, those signals were mixed and combined to drive a set of acousto-optic modulators designed to operate around 80 MHz, from which opposite diffraction orders were selected. The resulting modulation frequencies of the holograms (eq.12) were $\delta\omega_1 = \delta\omega'_1 + \delta\omega'_2$, $\delta\omega_2 = \delta\omega'_3$, $\delta\omega_3 = \delta\omega'_1 - \delta\omega'_2$. The three side band components \tilde{H}_{-1} , \tilde{H}_0 , and \tilde{H}_1 , encoded at 5 Hz, -2.5 Hz, and -7.5 Hz respectively, are visible on the magnitude of the discrete Fourier spectrum (eq. 12) reported in fig. 3. Spectral maps of the vibration amplitude $z_0(\omega)$ were calculated from a set of sequential measurements at each frequency. We took 3000 sequences of $N = 8$ raw interferograms \mathcal{I} at a readout rate of $\omega_S/(2\pi) = 20$ Hz, for excitation frequencies $\omega/(2\pi)$ ranging from 0 Hz to 3

kHz, in 1 Hz steps (supply voltage of the piezo electric actuator : 10 mV). The first resonance frequencies of the lamellophone's cantilevers are observed between 500 Hz and 2500 Hz (Media 1). In particular, a resonance of the first cantilever was identified around 541 Hz.

A finer screening around this resonance was performed, from 248 sequences of $N = 8$ raw interferograms, for excitation frequencies ranging from 536 Hz to 546 Hz (the values of $z_0(\omega)$ are reported in fig.4, points). But ψ_0 is randomized from one frequency point to the next. Hence the phase retardation ψ cannot be retrieved. To prevent reference phase randomization between measurements, a chirp of the frequency was performed. It consisted of a linear drift with time t of the excitation frequency from $\omega_I/(2\pi) = 536$ Hz to $\omega_F/(2\pi) = 546$ Hz in $T = 99.2$ s

$$\omega(t) = \omega_I + (\omega_F - \omega_I) t/T \quad (15)$$

Two out of the three components of the optical LO (eq. 8) were chirped as well via $\omega(t)$ throughout the acquisition. During the time lapse T , a sequence of $248 \times 8 = 1984$ raw interferograms \mathcal{I} was steadily recorded. Amplitude $z_0(\omega)$ and phase $\psi(\omega)$ maps at each frequency ω were calculated from the demodulation of $N = 8$ raw frame packets, reported in media 2. These maps were coherently averaged over the first cantilever according to eq. 13 and eq. 14 and reported in fig. 4 (blue lines). In agreement with eq.4, for non-zero viscosity, a phase shift of $\sim \pi$ is observed at the resonance frequency $\omega_r \sim 541.3$ Hz. The theoretical resonance lines in fig.4 were determined from values of ω_0 and ζ for which eq.3 and eq.4 best fit the experimentally-measured vibration amplitude.

In conclusion, we performed optical path length modulation imaging by time-averaged heterodyne holography in off-axis and frequency-shifting conditions. To do so, modulation side bands were acquired simultaneously through coherent frequency-division multiplexing. Additionally, a linear chirp of the excitation and the detection frequencies allowed to map the local mechanical phase retardation of a resonant cantilever with respect to the excitation signal without stroboscopy. The proposed method enabled robust and quantitative imaging of out-of plane nanometric vibration amplitudes.

We gratefully acknowledge support from Fondation Pierre-Gilles de Gennes (FPGG014), Agence Nationale de la Recherche (ANR-09-JCJC-0113, ANR-11-EMMA-046), région Île-de-France (C'Nano, AIMA), and the "investments for the future" program (LabEx WIFI: ANR-10-IDEX-0001-02 PSL*).

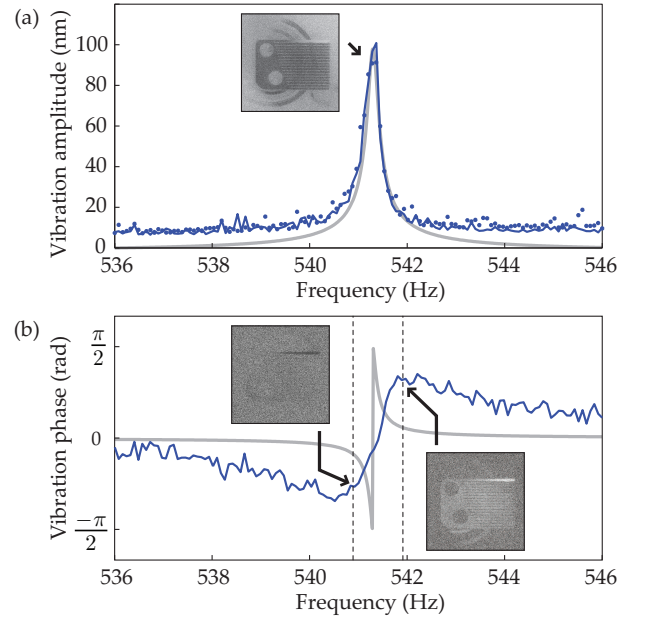


FIG. 4: Vibration amplitude z_0 (a) and phase ψ (b) averaged over the first cantilever, arrowed in fig. 2(b), versus excitation frequency $\omega/(2\pi)$. Insets : retrieved vibration amplitude and phase maps in the neighborhood of the resonance, reported in figs. 2(b,e,f). The points were obtained from a sequential measurement, the lines were obtained with the linear chirp (eq. 15). The theoretical resonance lines in gray were determined from eq.3 and eq.4.

[1] A. Bosseboeuf and S. Petitgrand. Characterization of the static and dynamic behaviour of MEMS by optical techniques: status and trends. *Journal of micromechanics and microengineering*, 13:S23, 2003.

[2] D. Royer and V. Kmetik. Measurement of piezoelectric constants using an optical heterodyne interferometer. *Electronics Letters*, 28(19):1828–1830, 1992.

[3] M. Leclercq, M. Karray, V. Isnard, F. Gautier, and P. Picart. Evaluation of surface acoustic waves on the human skin using quasi-time-averaged digital fresnel holograms. *Applied Optics*, 52(1):A136–A146, 2013.

[4] BM Watrasiewicz and P. Spicer. Vibration analysis by stroboscopic holography. *Nature*, 217:1142–1143, 1968.

[5] Ole J. Løkberg and Kåre Høgmoen. Vibration phase mapping using electronic speckle pattern interferometry. *Appl. Opt.*, 15(11):2701–2704, Nov 1976.

[6] S. Petitgrand, R. Yahiaoui, K. Danaie, A. Bosseboeuf, and JP Gilles. 3d measurement of micromechanical devices vibration mode shapes with a stroboscopic interferometric microscope. *Optics and lasers in engineering*, 36(2):77–101, 2001.

[7] Julien Leval, Pascal Picart, Jean Pierre Boileau, and Jean Claude Pascal. Full-field vibrometry with digital fresnel holography. *Appl. Opt.*, 44(27):5763–5772, Sep 2005.

[8] M. Atlan, M. Gross, and N. Verrier. Phase-resolved heterodyne holographic vibrometry with a strobe local oscillator. *arXiv preprint arXiv:1211.5428*, 2012.

[9] Giancarlo Pedrini, Wolfgang Osten, and Mikhail E. Gusev. High-speed digital holographic interferometry for vibration measurement. *Appl. Opt.*, 45(15):3456–3462, May 2006.

[10] C. PÚrez-Lpez, M.H. De la Torre-Ibarra, and F. Mendoza Santoyo. Very high speed cw digital holographic interferometry. *Optics Express*, 14(21):9709–9715, 2006.

[11] R. L. Powell and K. A. Stetson. Interferometric vibration analysis by wavefront reconstruction. *J. Opt. Soc. Am.*, 55:1593, 1965.

[12] C. C. Aleksoff. Time average holography extended. *Appl.*

- Phys. Lett.*, 14:23, 1969.
- [13] Karl A. Stetson. Effects of beam modulation on fringe loci and localization in time-average hologram interferometry. *J. Opt. Soc. Am.*, 60(10):1378, 1970.
 - [14] JA Levitt and KA Stetson. Mechanical vibrations: mapping their phase with hologram interferometry. *Applied Optics*, 15(1):195–199, 1976.
 - [15] M. Paturzo, P. Memmolo, A. Tulino, A. Finizio, and P. Ferraro. Investigation of angular multiplexing and demultiplexing of digital holograms recorded in microscope configuration. *Opt. Express*, 17(11):8709–8718, 2009.
 - [16] Tomohiro Kiire, Daisuke Barada, Jun ichiro Sugisaka, Yoshio Hayasaki, and Toyohiko Yatagai. Color digital holography using a single monochromatic imaging sensor. *Opt. Lett.*, 37(15):3153–3155, Aug 2012.
 - [17] Tatsuki Tahara, Akifumi Maeda, Yasuhiro Awatsuji, Takashi Kakue, Peng Xia, Kenzo Nishio, Shogo Ura, Toshihiro Kubota, and Osamu Matoba. Single-shot dual-illumination phase unwrapping using a single wavelength. *Opt. Lett.*, 37(19):4002–4004, Oct 2012.
 - [18] N. Verrier and M. Atlan. Absolute measurement of small-amplitude vibrations by time-averaged heterodyne holography with a dual local oscillator. *arXiv preprint arXiv:1211.5328*, 2012.
 - [19] Etienne Cuhe, Pierre Marquet, and Christian Depeursinge. Spatial filtering for zero-order and twin-image elimination in digital off-axis holography. *Applied Optics*, 39(23):4070, 2000.